IOP Conf. Series: Materials Science and Engineering **443** (2018) 012038 doi:10.1088/1757-899X/443/1/012038

Domain structure imaging in PMN-PT crystals using channelling-contrast backscattered electron microscopy

E O Vlasov[1], D S Chezganov[1], L V Gimadeeva[1], A D Ushakov[1], Q Hu[2], X Wei[2] and V Ya Shur[1]

[1] School of Natural Sciences and Mathematics, Ural Federal University, 620000, Ekaterinburg, Russia
[2] Electronic Materials Research Laboratory, Key Laboratory of the Ministry of Education & International Centre for Dielectric Research, Xi'an Jiaotong University, 710049, Xi'an, China

evgeny.vlasov@urfu.ru

Abstract. We demonstrate the abilities of various SEM techniques for domain imaging in PMN-PT crystals with different compositions. It is shown that the imaging of the chemically etched relief is limited by its destructivity and potential contrast – by low resolution and contrast instability. The optimal parameters of the imaging by backscattered electron channelling allow obtaining the high-resolution domain imaging in PMN-PT crystals. The domain structure change as a result of the phase transition are imaged. The correlation between the images of the surface domain structure obtained by scanning electron microscopy and piezoresponse force microscopy is demonstrated.

1. Introduction

The lead magnesium niobate-lead titanate $(1-x)Pb(Mg_{1/3}Nb_{2/3})O_3$-$xPbTiO_3$ (PMN-PT) crystals are well known for their outstanding physical properties, such as high electromechanical and piezoelectric coefficients, high strain, and low dielectric losses [1,2]. It makes PMN-PT crystals promising for various applications including ultrasonic transducers, piezoelectric actuators, etc. Moreover, PMN-PT is a potential candidate for non-linear optics and photonics.

The domain imaging by several microscopic techniques with a high spatial resolution is important for studying the domain structure produced by various treatments [3-5]. The domain imaging by scanning electron microscopy (SEM) possesses high resolution and comparatively fast image acquisition. The method can be used in wide temperature range and allows visualizing slow domain evolution [6]. SEM was used for imaging of the domain structure of bulk ferroelectric single crystals [7-10], ceramics [11,12], and thin films [13]. The imaging was realized via several techniques, such as visualization of etched domains [10,14], secondary electron imaging (potential contrast) [7,15], electron beam stimulated polarization currents [9], electron backscatter diffraction [16], and secondary and backscattered electron imaging using electron channelling [6,11,17-19].

The backscattered electron (BSE) mode via electron channelling is a relatively simple technique with resolution below 10 nm. BSE represents primary electrons, which after experiencing one or multiple scatterings in the sample, eventually emerge from the surface. Two types of BSE are distinguished: (1) high angle BSE as a result of Rutherford scattering and (2) low angle BSE realized by Mott scattering. The first one carries information about atomic number, while the second one is

sensitive to the surface orientation. The domain contrast is based on the channelling of incident electron beam within domains of different orientations, which modulates the BSE emission and provides a contrast caused by crystallographic orientation. The method was applied for studying the domain structure change under mechanical stress [6,17] and electric field [18,19] in wide temperature range. Moreover, the electron channelling contrast is a powerful technique for imaging crystal defects, such as dislocations, stacking faults, twins, and grain boundaries [20].

In this paper, we demonstrate the first successive application of the BSE channelling mode for the domain imaging in PMN-PT crystals.

2. Experimental

We used the field emission scanning electron microscope (FE-SEM) Merlin (Carl Zeiss NTS GmbH) with Schottky field emitter. The domain structures were visualized using four quadrant angular selective BSE detectors with accelerating voltage 1-20 kV and electron beam current from 100 pA to 2 nA.

We studied the PMN-PT crystals grown by modified Bridgman technique of various compositions with different phases at the room temperature: rhombohedral (R), tetragonal (T), and morphotropic phase boundary (MPB) [21]. The following procedure was used for sample preparation: (1) polishing by water suspension of diamond particles with sizes down to 1 μm and (2) mechanochemical polishing with silica compound SF1 suspension to remove residual deformation and amorphous surface layer. The samples were mounted on a holder by a conductive sticky tape. In order to remove excess charge induced by electron beam, the samples were covered by 6-nm-thick carbon layer.

3. Results and discussion

We checked the abilities of the most common methods of domain imaging for PMN-PT. It is well known that the combination of the selective chemical etching and SEM allows visualizing the domain structures with a resolution down to 2 nm. We applied this method to PMN-PT single crystals. Thus, we obtained the topography corresponding to the domain structure revealed after mechanochemical polishing with a colloidal silica (Fig. 1a,b). The technique revealed the maze domain structures with a characteristic width of 0.5-2 μm (Fig. 1a) and needle-like structures with a width down to 150 nm (Fig. 1b).

We used the potential contrast in order to visualize domain structure and observed mentioned above obstacles, such as low resolution and stability (Fig. 1c). Moreover, surface charging caused by electron beam scanning led to disappearance of the surface potential contrast due to screening.

In order to define optimal parameters for domain imaging by channelling contrast, we studied the dependence of domain contrast and resolution on accelerating voltage (primary electron beam energy), electron beam current, and working distance (distance from the pole piece of the electron column to the sample surface). It was shown that decrease of working distance increased the resolution and domain contrast due to increase of the solid angle of the electron beam, and BSE detection resulted in prevailed detection of the low angle BSE. The increase of the accelerating voltage also increased the

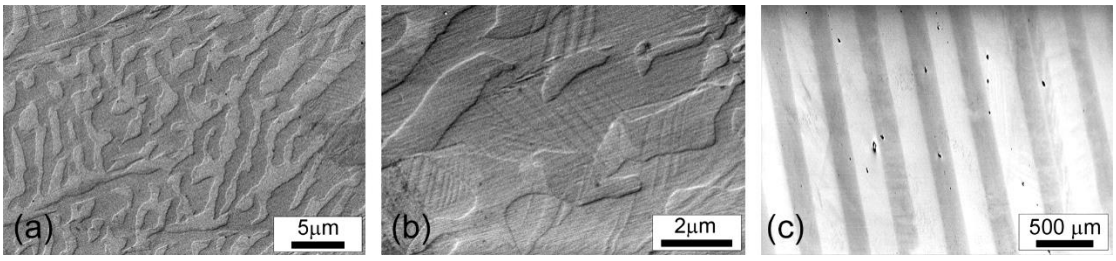

Figure 1. SEM images of the domain structures in PMN-PT crystals: (a,b) domains revealed by selective chemical etching during mechanochemical polishing, (c) potential contrast of *a*-domains.

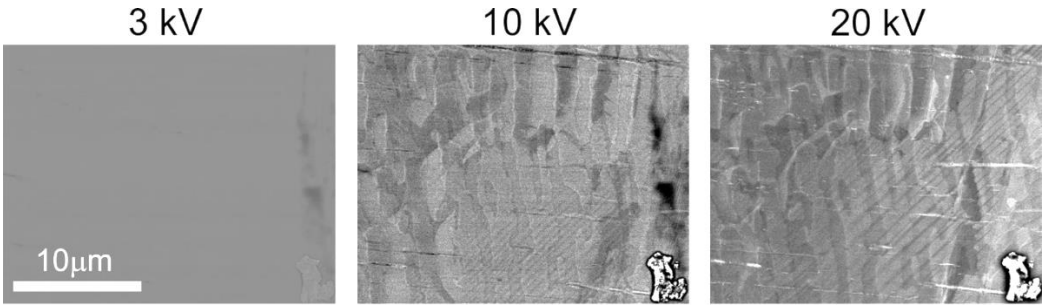

Figure 2. SEM images of the domain structures in PMN-PT crystals at various accelerating voltages in electron channelling mode.

resolution and the domain contrast (Fig. 2) due to reduction of the electron probe size and increase of the interaction volume. It should be noted that the presence of the damaged surface layer formed during polishing, hampered the domain imaging at low electron energies. It was demonstrated that rise of the beam current enhanced the contribution of the topography contrast due to the increase of the SE quantity, which could be detected at the same time by BSE detector. Thus, the optimal parameters were revealed (Table 1).

It was shown that the electron beam scanning during the image acquisition might lead to the change of the initial domain state (Fig. 3) caused by generation of the electric field induced by the charge accumulation. This issue can be overcome by deposition of the surface conductive layer. Deposition of the 6-nm-thick carbon layer allowed removing the charging effect and keeping the domain contrast.

Table 1. Optimal parameters for domain imaging using channelling contrast in PMN-PT crystals.

Parameter	Value
Working distance (mm)	below 4
Accelerating voltage (kV)	above 20
E-beam current (pA)	about 0.3

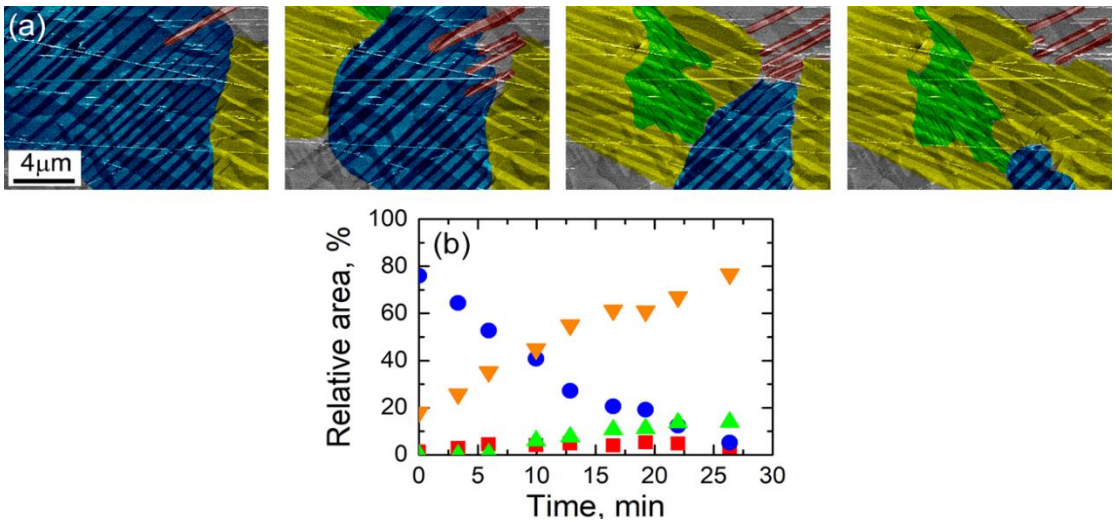

Figure 3. (a) SEM images of the domain structures in PMN-PT crystals obtained by sequential scanning. Scanning time is 3 min, (b) time dependence of the relative area for each domain type.

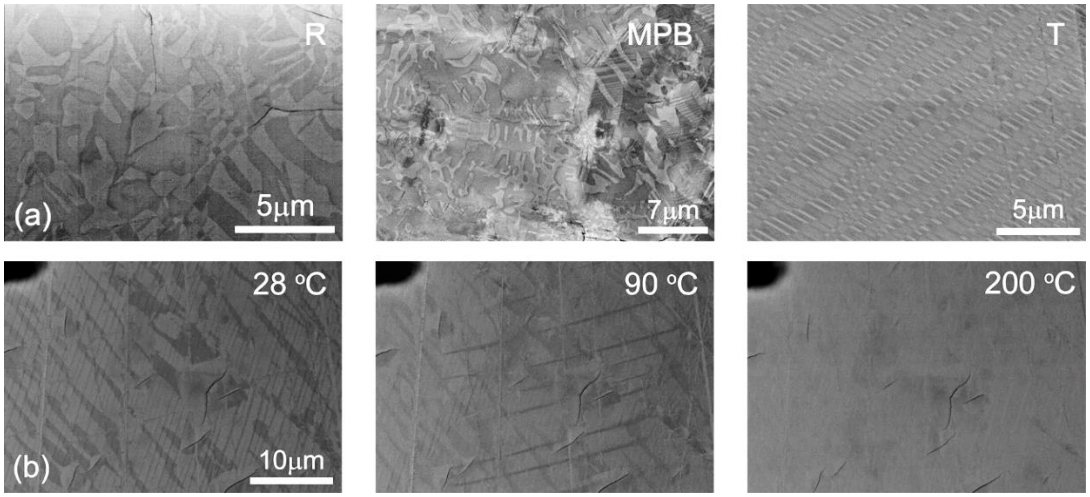

Figure 4. SEM images of the domain structures in PMN-PT crystals obtained: (a) for various compositions, (b) at the different temperatures.

We used the obtained information to visualize the nanodomain structures in PMN- PT in rhombohedral and tetragonal phases and the composition corresponding to the MPB region (Fig. 4a). Moreover, we demonstrated the ability to image the domain structure change as a result of the phase transition during the temperature treatment in 0.67PMN-0.33PT crystals (Fig. 4b). Two types of as-grown domain structures: quasi-regular patterns of pin-stripe domains and the laminar domains were visualized at the room temperature. The heating up to 70°C led to disappearing of the pin-stripe domains and formation of the long needle-like domains. Such behaviour can be attributed to the transition from monoclinic to tetragonal phase. Further heating above 200°C resulted in domain disappearance due to transition to the paraelectric phase.

The good correlation between domain images obtained in MPB phase of PMN-PT crystals by piezoresponse force microscopy (PFM) and SEM in channelling mode (Fig. 5) was demonstrated. The better quality of SEM images can be attributed to the difference in depth of the obtained signal: tens of nanometres for SEM and above micron for PFM. It should be noted that, the image acquisition time for SEM is essentially shorter. It makes the SEM channelling mode more attractive as compared with PFM.

4. Conclusion

The abilities of various SEM techniques for domain imaging were demonstrated in PMN-PT crystals with different compositions. It was shown that the imaging of the chemically etched relief was limited by its destructivity and potential contrast – by low resolution and contrast instability. The channelling

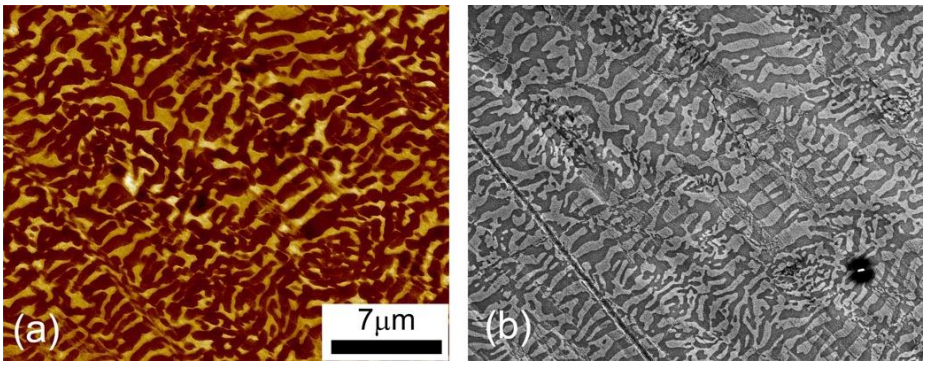

Figure 5. Domain images of the MPB PMN-PT crystals obtained by: (a) PFM, (b) SEM.

mode BSE detection looks preferable. The optimal parameters of the BSE channelling imaging were obtained. The high-resolution domain imaging in PMN-PT crystals in rhombohedral and tetragonal phases and the composition corresponding to the morphotropic phase boundary region were shown. The domain structure change as a result of the phase transition was imaged. The comparison of SEM and PFM domain images showed good correlation.

Acknowledgments
The equipment of the Ural Centre for Shared Use "Modern Nanotechnology" Ural Federal University has been used. The research was made possible by RFBR (grant 17-52-80116-BRICS_a) and state task of Ministry of education and science of the Russian Federation (No. 3.4993.2017/6.7). The work was partially supported by Government of the Russian Federation (Act 211, Agreement 02.A03.21.0006).

References
[1] Park S-E and Shrout T R 1997 *J. Appl. Phys.* **82** 1804-11
[2] Zhang R, Jiang B and Cao W 2001 *J. Appl. Phys.* **90** 3471-5
[3] Soergel E 2005 *Appl. Phys. B* **81** 729-51
[4] Tagantsev A K, Cross L E and Fousek J 2010 *Domains in Ferroic Crystals and Thin Films* (New York: Springer)
[5] Potnis P, Tsou N-T and Huber J 2011 *Materials* **4** 417-47
[6] Reichmann A, Zankel A, Reingruber H, Pölt P and Reichmann K 2011 *J. Eur. Ceram. Soc.* **31** 2939-42
[7] Le Bihan R 1989 *Ferroelectrics* **97** 19-46
[8] Zhu S and Cao W 1997 *Phys. Rev. Lett.* **79** 2558-61
[9] Sogr A A and Kopylova I B 1997 *Ferroelectrics* **191** 193-8
[10] Kuznetsov D K, Chezganov D S, Mingaliev E A, Kosobokov M S and Shur V Y 2016 *Ferroelectrics* **503** 60-7
[11] Gruner D and Shen Z 2010 *J. Am. Ceram. Soc.* **93** 48-50
[12] Omori M, Mishima T and Fujimoto T 2011 *Jpn. J. Appl. Phys.* **50** 09NC03
[13] Ihlefeld J F, Michael J R, McKenzie B B, Scrymgeour D A, Maria J-P, Paisley E A and Kitahara A R 2017 *J. Mater. Sci.* **52** 1071-81
[14] Robinson G Y and White R M 1967 *Appl. Phys. Lett.* **10** 320-3
[15] Kokhanchik L S 2018 *Phys. Solid State* **60** 1778-85
[16] Howell J A, Vaudin M D and Cook R F 2014 *J. Mater. Sci.* **49** 2213-24
[17] Karlsen M, Einarsrud M-A, Lein H L, Grande T, Hjelen J and Vullum P E 2009 *J. Am. Ceram. Soc.* **92** 732-7
[18] Leach C, Ali N K and Hall D A 2011 *Ceram. Int.* **37** 2185-91
[19] Otonicar M, Reichmann A and Reichmann K 2016 *J. Eur. Ceram. Soc.* **36** 2495-504
[20] Zaefferer S and Elhami N-N 2014 *Acta Mater.* **75** 20-50
[21] Wang R, Xu H, Yang B, Luo Z, Sun E, Zhao J, Zheng L, Dong Y, Zhou H, Ren Y, Gao C and Cao W 2016 *Appl. Phys. Lett.* **108** 152905